Water Landing Impact of Recovery Space Capsule:
A Research Overview

Eiichiro NAKANO[1], Hideaki UCHIKAWA[1], Hideyuki TANNO[2], Ryu SUGIMOTO[3],

[1] Japan Aerospace Exploration Agency (JAXA), 2-1-1, Sengen, Tsukuba-shi, Ibaraki, 305-8505 Japan
[2] Japan Aerospace Exploration Agency (JAXA), 1 , Koganesawa, Kimigaya, Kakuda-shi, Miyagi, 981-1525 Japan
[3] Mitsubishi Space Software Co., Ltd., Tsukuba Mitsui Bldg., 1-6-1, Takezono, Tsukuba-shi, Ibaraki, 305-0032 Japan

TEL / FAX: +81-50-3362-4169 / +81-29-868-3950
E-mail: nakano.eiichiro@jaxa.jp

ABSTRACT

For the design of a manned or cargo space capsule, it is important to precisely estimate the Earth landing loads to the crew or cargo, and to limit the loads to within a permissible range. Water landing simulations and scale-model water landing tests with varying conditions for descending velocity, pitch angle, and horizontal velocity during splashdown were conducted to estimate the magnitude of water impact on the recovery space capsule. This paper describes the results of the simulation and water landing tests.

1. INTRODUCTION

JAXA is making progress on both the HTV-R study (H-II Transfer Vehicle – Return), which adds cargo recovery function to the HTV (H-II Transfer Vehicle), and a concept study of the future Japanese manned space capsule. The Earth landing concepts are water landing for HTV-R, and water or land landing for the future manned capsule. In either case, it is indispensable for recovery space capsule to precisely estimate the level of impact on cargo or crew, and to attenuate the impact below the permissible level specified during the design phase. This paper gives an overview of the water landing simulation of the capsule and test results.

In order to evaluate water landing impact on the recovery space capsule, the following studies are needed: (1) estimate the magnitude of impact to the vehicle, (2) understand the characteristics of impact transmission/attenuation from vehicle to interface point (e.g., crew seating), (3) establish methods to assess the load to human body, and (4) set a design threshold that should not exceed at the interface point (Fig. 1). The first phase of this research is to estimate changes in water landing impact based on vehicle shape and landing condition (e.g., landing velocity and pitch angle). Computer simulation and scale-model water landing tests with varying conditions for pitch angle, vertical velocity, and horizontal velocity were conducted using the HRV (HTV Return Vehicle) baseline configuration (reentry capsule portion of HTV-R) (Fig. 2, Ref. 1).
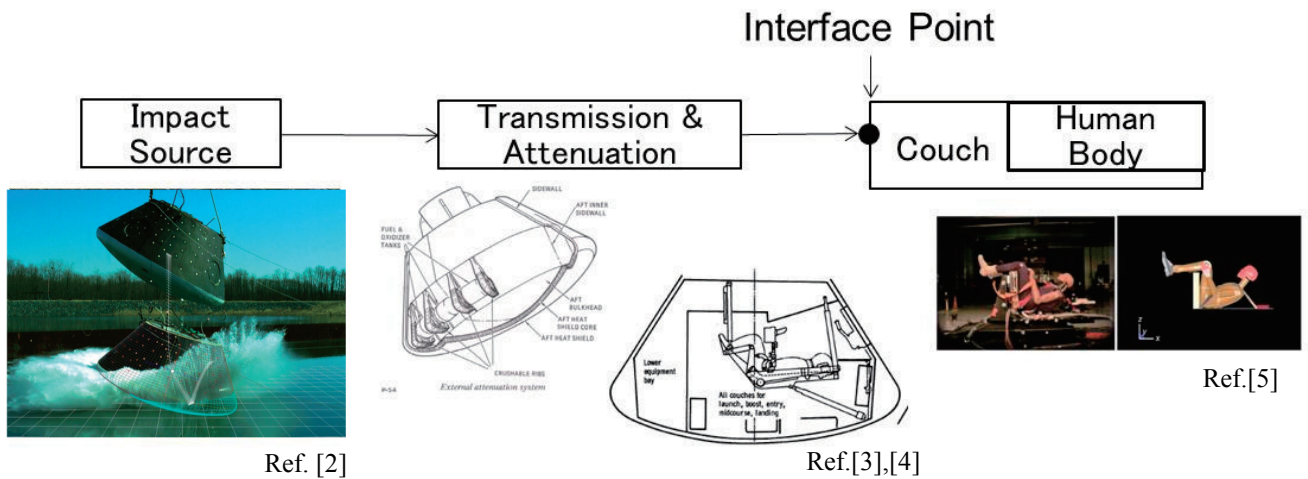
Fig. 1. Load flow from water landing impact to human body

Fig. 2. HRV (HTV Return Vehicle)

2. WATER LANDING SIMULATION

MSC-Dytran, an explicit finite element analysis code, was used in the water landing simulation. The HRV vehicle model was used in this simulation and was assumed as rigid body (Fig. 3). Simulation conditions were 5-20 m/s vertical velocity and 0-30° pitch angles (Ref. 6, 7), and accelerations of the vehicle's center of gravity are shown in this section.
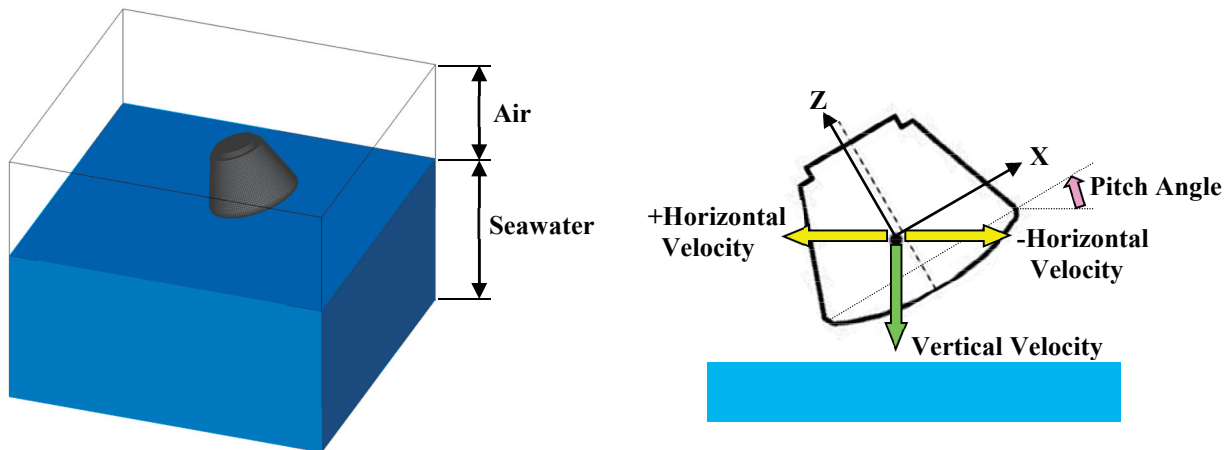

Fig. 3. Water Landing Simulation Model

Maximum accelerations to vertical velocity at 0, 10, 20, and 30° pitch angles are shown in Fig. 4. The maximum accelerations parabolically increase as the vertical velocity increases. Fig. 5 shows maximum accelerations to pitch angle at 5-20 m/s vertical velocity. The maximum Z-acceleration is higher at 0-10° pitch angle, and the maximum X-acceleration is higher at 10-20° pitch angle. Maximum accelerations are relatively lower at 25-30° pitch angle, which is desirable for decreasing the water impact load.
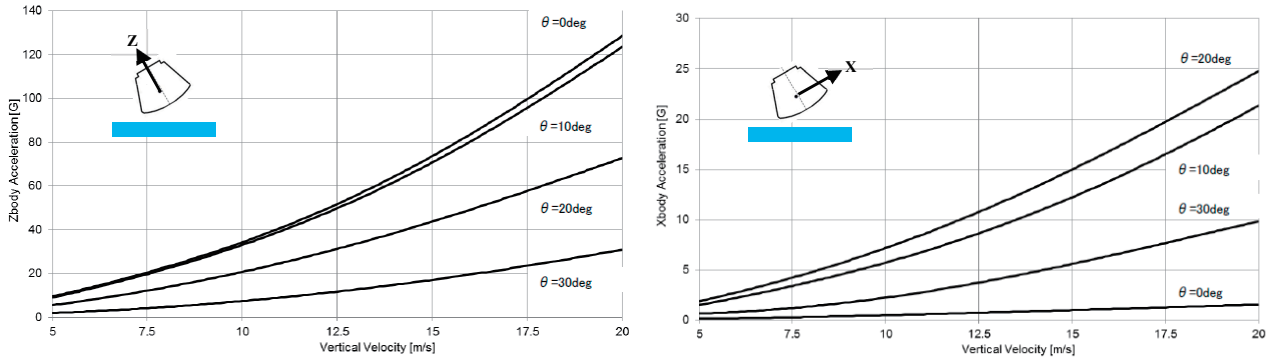
Fig. 4. Maximum Z, X-acceleration to vertical velocity at 0, 10, 20 and 30° pitch angles
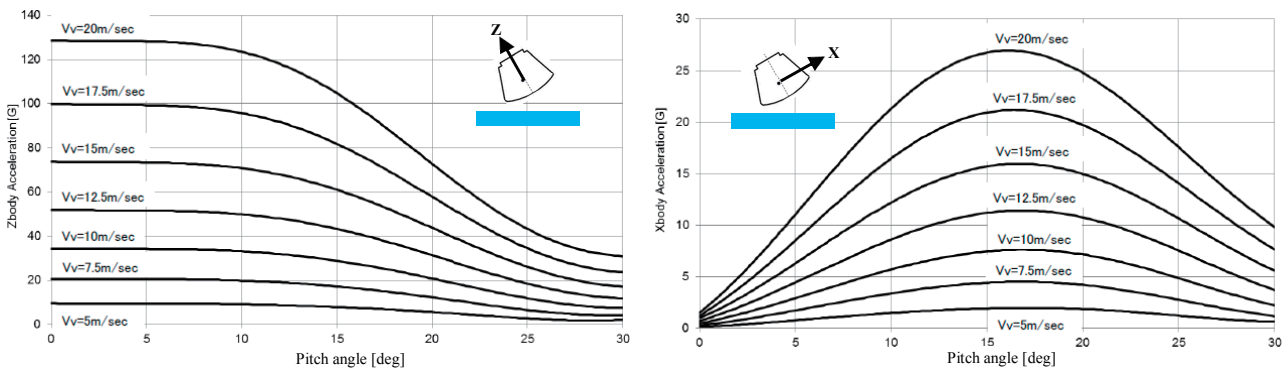
Fig. 5. Maximum Z, X-acceleration to pitch angle at 5-20 m/s vertical velocity

Maximum accelerations to horizontal velocity at 30° pitch angle and at 10 m/s vertical velocity are shown in Fig. 6. Maximum Z-acceleration increases as horizontal velocity decreases, while X-acceleration increases as horizontal velocity increases.
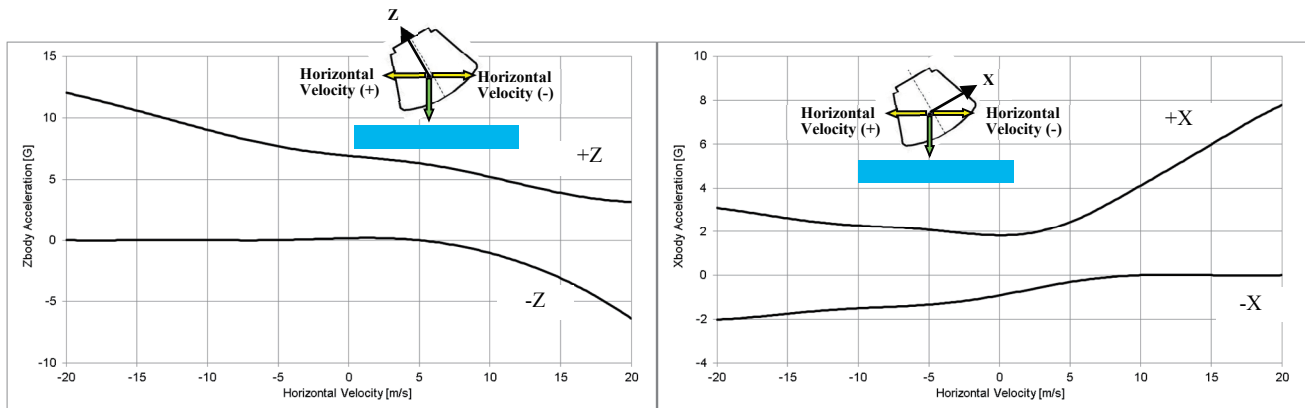
Fig. 6. Maximum Z, X-acceleration to horizontal velocity at 10 m/s vertical velocity and 30° pitch angle

Z-accelerations to time after splashdown of a full-scale simulation and 6.8%-model simulation are shown in Fig. 7. The full-scale simulation had a 30° pitch angle and 15m/s vertical velocity. The 6.8%-model simulation had a 30° pitch angle and 3.9 m/s vertical velocity, with the same Froude number as the full-scale condition. Although both results share a similar profile, data oscillation was observed for the model-scale simulation.

3. WATER LANDING TEST

3.1 6.8% scaled water landing capsule model

Fig. 7. Z-acceleration to time after splashdown at full-scale condition of 30º pitch angle and 15 m/s vertical velocity

A 6.8% scale-model of HRV was constructed for the water landing test (Fig. 8, Ref. 8). The model has a maximum diameter of 285.6 mm, with mass and center of gravity that fits the full-scale HRV (Fig. 2). The model was painted in yellow and black checkered pattern for image analysis.

A miniature data-logger, developed at JAXA Kakuda Space Center (Ref. 9), and accelerometers were installed in the model to obtain water landing test data without cable connections. Sampling rate of the data logger was 10 kHz and PCB Piezotronics 352C65 (measurement range, ±50g pk) or 352A21 (measurement range, ±500 g pk) accelerometers were installed.

Fig. 8. 6.8% scale model of HRV for the water landing test

3.2 Water Landing Test Method

A water tank of 2.1 m diameter and 0.45 m depth was used for the test. Test data from both small-scale test tank and large test tank (50 m length, 8 m width, 4.5 m depth) were compared. Acceleration in the small tank was slightly higher than in the large tank at small pitch angles of 0-10º. However, accelerations were approximately equal in both tanks at 30º pitch angle. The small test tank was used in this study to facilitate testing of horizontal velocity.

Table 1. Froude scaling laws

	Full-scale Value	Scale Factor	Model Value
Length	L	λ	λL
Mass	m	λ^3	$\lambda^3 m$
Moment of inertia	I	λ^5	$\lambda^5 I$
Time	t	$\lambda^{1/2}$	$\lambda^{1/2} t$
Velocity	v	$\lambda^{1/2}$	$\lambda^{1/2} v$
Linear acceleration	a	1	a
Angular acceleration	α	λ^{-1}	$\lambda^{-1}\alpha$

The test was performed with varying pitch angles, vertical velocities, and horizontal velocities of the model during splashdown. Based on the Apollo command module's nominal pitch angle (27.5º)
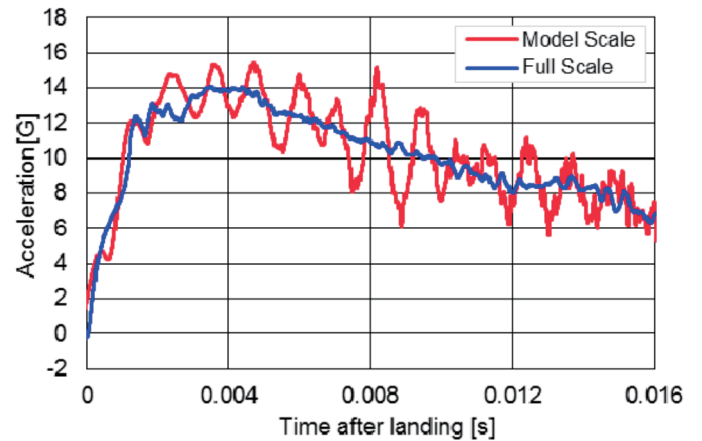
and vertical velocity (9.1 m/s) (Ref. 10), nominal water landing conditions, 30º pitch angle and 10 m/s vertical velocity, were initially chosen for the HRV. Conditions for the 6.8% scale-model test were 30º pitch angle and 2.6 m/s vertical velocity based on Froude scaling laws (Table 1).

In the vertical landing test, the model was dropped vertically. In the landing test with horizontal velocity, the model was dropped using a sliding table or a swing like pendulum (Fig. 9).

In addition to acquisition of internal accelerometer data, motion images of water landing tests were recorded at 1000 frames/sec. Velocity and acceleration of the model were computed using motion image analysis software.
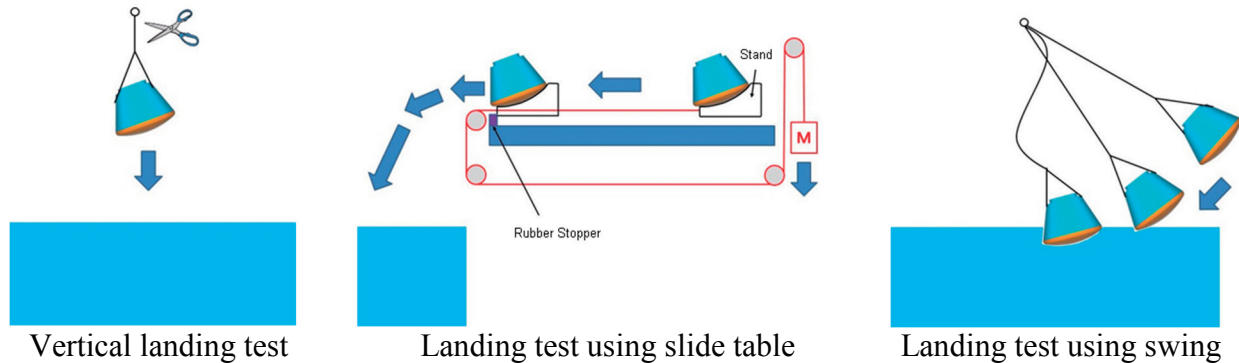

| Vertical landing test | Landing test using slide table | Landing test using swing |

Fig. 9. Water landing test

3.3 Test results

Maximum accelerations to pitch angle at 2.6 m/s vertical velocity, which is equivalent to approximately 10 m/s in full-scale size, are shown in Fig. 10. Accelerations at the bottom center of the model were measured in this section. Maximum Z-acceleration values were observed at 0-10º pitch angle, decreasing as the pitch angle increased, and dropped to below 10g at 25-35º pitch angle. X-accelerations were -5-0g at all pitch angles. Both accelerometer and motion image analysis data are shown in Fig. 10. Regarding accelerometer, data below 20º pitch angle were unavailable due to oscillating of the model's bottom.

Maximum accelerations to vertical velocity at pitch angles of 0, 10, 20 and 30º are shown in Fig. 11. Z-acceleration values decreased with increase in pitch angle. Absolute values for X acceleration were highest at 20º pitch angle, while smallest at 0º pitch angle.
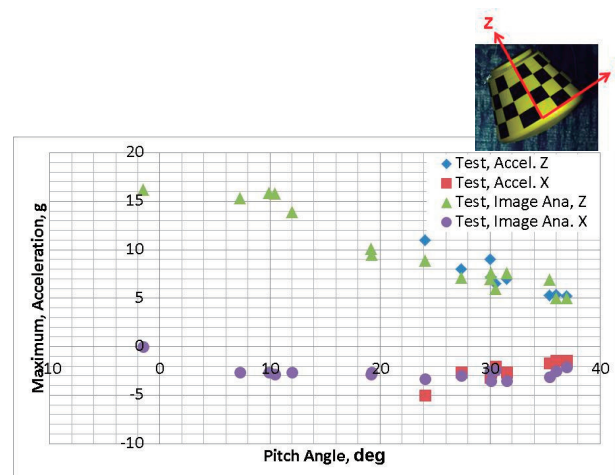

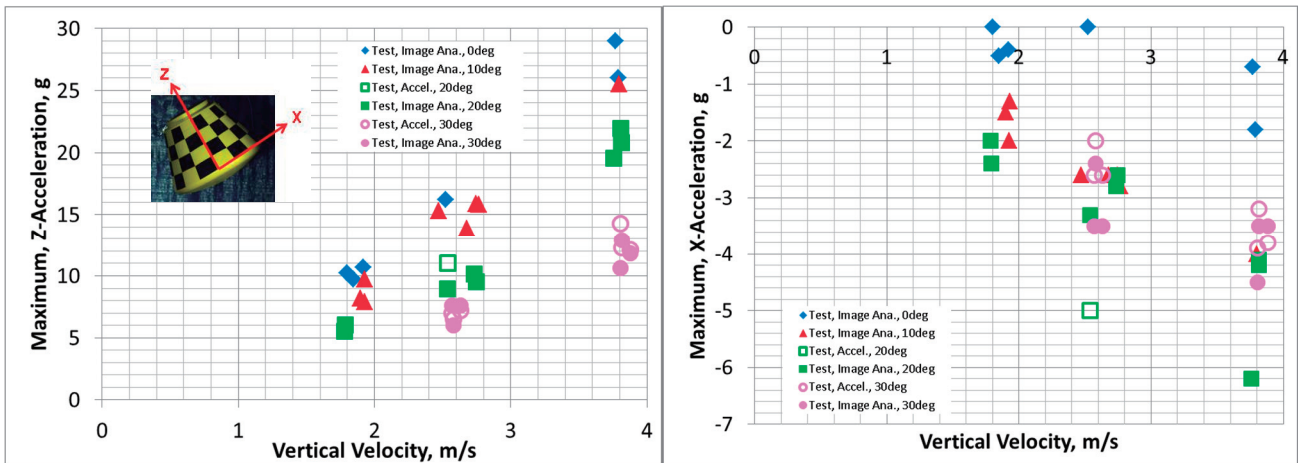Fig. 10. Maximum accelerations to pitch angle at 2.6m/s vertical velocity

Fig. 11. Maximum accelerations of vertical velocity at the pitch angle of 0, 10, 20 and 30°

Fig. 12 shows the maximum accelerations to horizontal velocity at 2.6 m/s vertical velocity (equivalent to approximately 10 m/s for full-scale) and at 30° pitch angle. Maximum accelerations for Z at minus and zero horizontal velocity are 5-8g, and are 4g for plus horizontal velocity. This is probably because the model at plus horizontal velocity condition drops from the outermost peripheral part with small radius of curvature.

4 COMPARISON BETWEEN SIMULATION AND TEST RESULTS

Comparison between simulation results and water impact test results are described in this section. Maximum accelerations to pitch angle at 10m/s vertical velocity on simulation and about 2.6 m/s on water impact test (equivalent to approximately 10 m/s for full-scale) are shown in Fig. 13. As in section three, accelerations at the bottom center of the model are shown in this section. Maximum accelerations to vertical velocity at 0, 10, 20 and 30° pitch angles are shown in Fig. 14. Although simulation and test results at 30° pitch angle showed good agreement, test accelerations from motion image analysis at lower pitch angles were lower than simulation data and illegible or excessive accelerations were obtained from accelerometers installed inside the model. Motion image analysis was performed on 1000 frames per second images, which was too low to calculate acceleration. Accelerometers were installed on the model's bottom shell plate
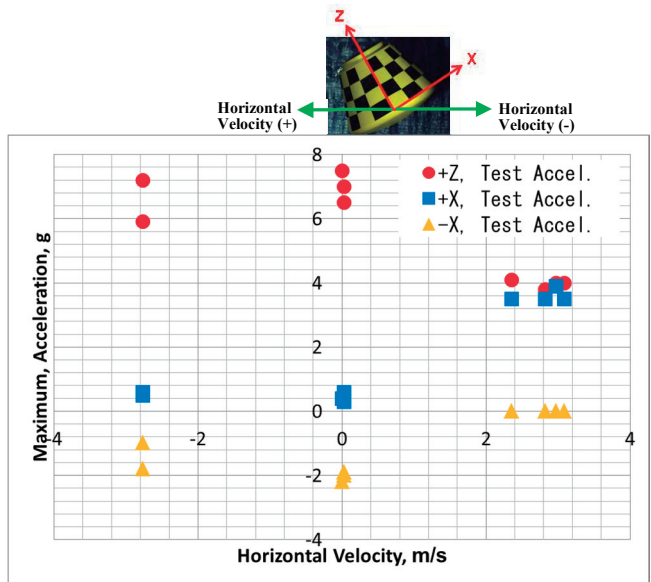

Fig. 12. Maximum accelerations to horizontal velocity at 2.6m/s vertical velocity and 30° pitch angle
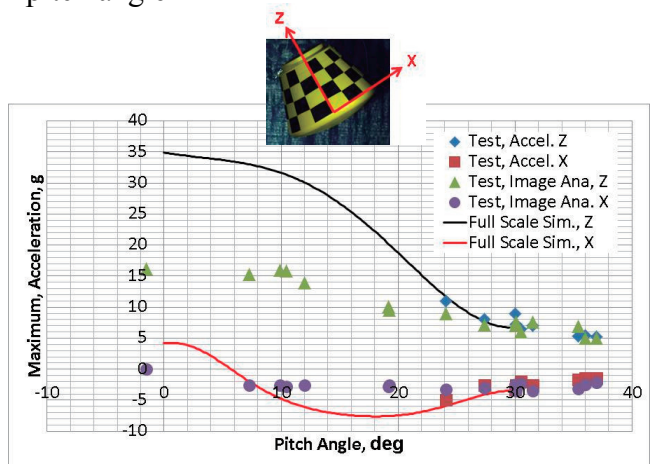

Fig. 13. Comparison between full-scale simulation and 6.8%-model test results – maximum accelerations to pitch angle at 10 m/s vertical velocity for full-scale

for this test. However, these needed to be installed far from the model's bottom, or the model's bottom shell plate needed to be thickened more.

Maximum accelerations to horizontal velocity at 10m/s vertical velocity for full-scale and at 30° pitch angle are shown in Fig. 15. These values showed good agreement.
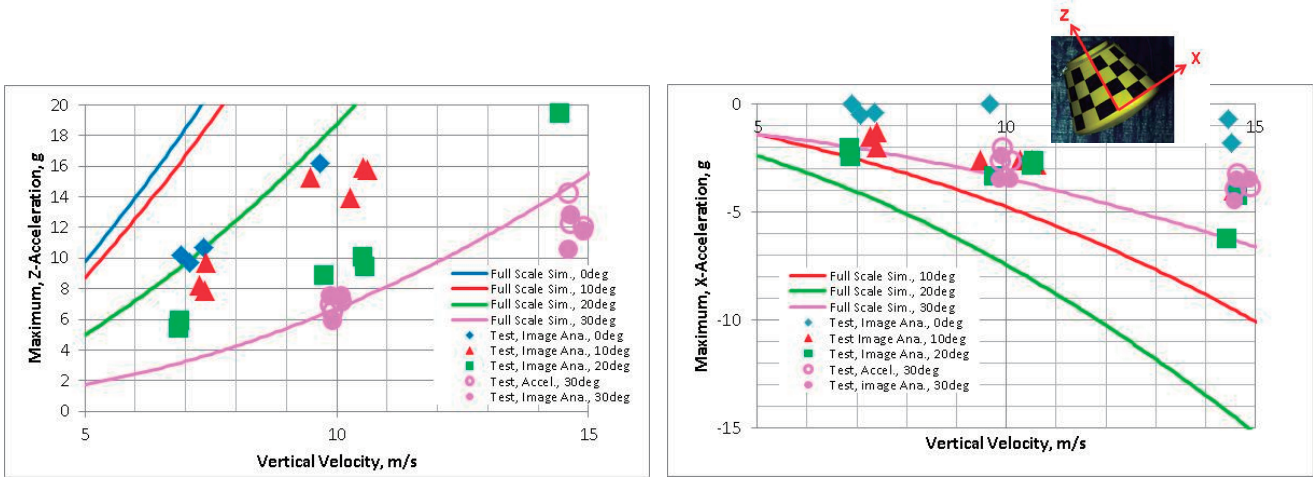

Fig. 14. Comparison between full-scale simulation and 6.8%-model test results - maximum accelerations to vertical velocity at 0, 10, 20 and 30° pitch angle
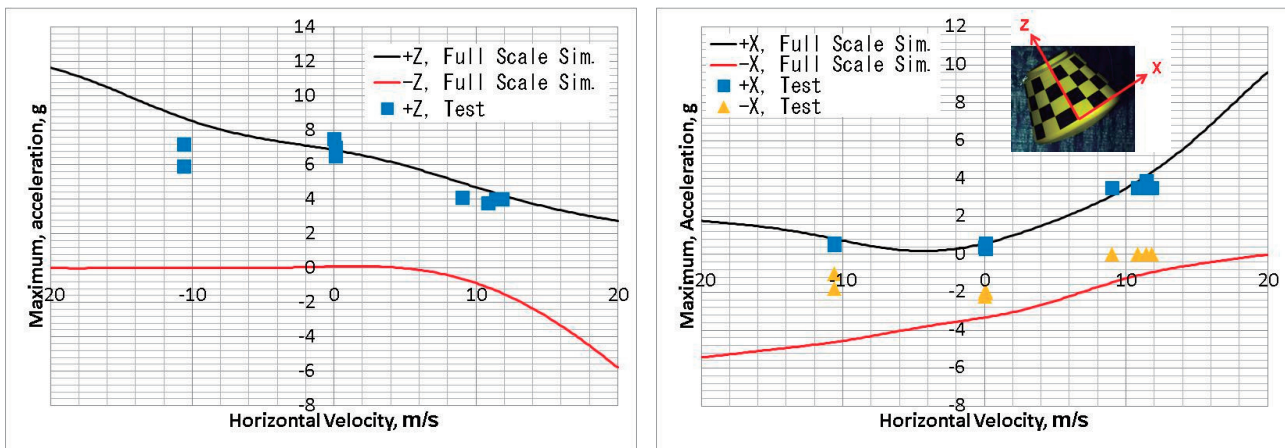

Fig. 15. Comparison between full-scale simulation and 6.8%-model test results – maximum accelerations of horizontal velocity at 10m/s vertical velocity for full-scale and at 30° pitch angle

Time series for Z accelerations of 6.8%-scale simulation and 6.8%-model test at 30° pitch angle, 2.6m/s vertical velocity (equivalent to 10 m/s for full-scale) and -2.6 m/s horizontal velocity (equivalent to -10 m/s for full-scale) is shown in Fig. 16. Although the 6.8%-scale simulation showed oscillating data, most values showed good agreement.

5 CONCLUSION

This paper describes results for the water landing simulation and tests of recovery space capsule. The maximum acceleration during splashdown for the capsule pitch angle of
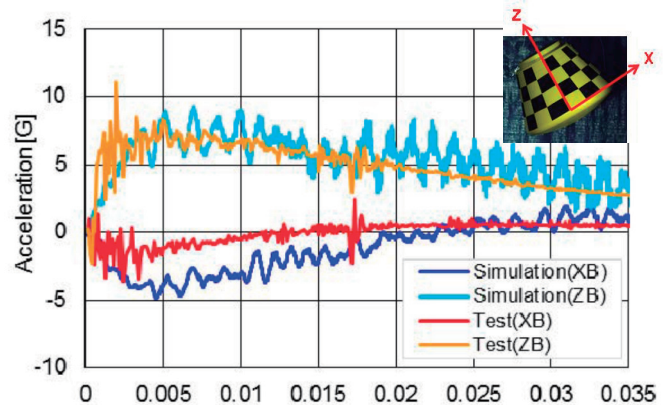

Fig. 16. Comparison between 6.8%-scale simulation and 6.8%-model test results – Z accelerations to time after landing at 30° pitch angle, 2.6 m/s vertical velocity and -2.6 m/s horizontal velocity for 6.8%-scale

30°and vertical velocity (descending velocity) of 10 m/s, which are nominal conditions for full-scale HRV water landing, were below 10g in the axial Z direction. At this condition, simulation and test results showed good agreement. Test accelerometer results at pitch angles below 30° were unreadable or too high, and image analysis results were low compared with simulation results. The test model and/or measurement methods need to be improved for future testing. Trends in maximum acceleration to pitch angle, vertical velocity and horizontal velocity were observed.

As described in section two, this paper presents the first phase of our research, which is to estimate the magnitude of impact to the vehicle during water landing. In the future, we will also evaluate the impact during land landing, investigate the characteristics of impact transmission/attenuation to the vehicle and assess the load to the human body. We would like to progress this research, referring the research of not only manned space vehicle but also automobile crash, etc.

ACKNOWLEDGMENTS

REFERENCES

[1] Y. Suzuki and T. Imada, "Concept and Technology of HTV-R: An Advanced Type of H-II Transfer Vehicle", 28th ISTS, 2011-g-09, 2011.
[2] T. Jones, T. Johnson, D. Shemwell and C. Shreves, "Photogrammetric Technique for Center of Gravity Determination", AIAA2012-1882, 2012.
[3] J. McCullough and J. Lands, "Apollo Command Module Land-Impact Tests", NASA TN D-6979, 1972.
[4] R. Drexel and H. Hunter, "Apollo Experience Report - Command Module Crew-Couch/Restraint and Load-Attenuation Systems", NASA TN D-7440, 1973.
[5] A. Taniei, C. Lawrence and E. Fasanella, "Validation of Finite Element Crash Test Dummy Models for Predicting Orion Crew member Injuries During a Simulated Vehicle Landing", NASA/TM-2009-215476, 2009.
[6] E. Nakano, H. Uchikawa, H. Tanno, H. Akagi, T. Seki, T. Shimoda and R. Sugimoto, "Overview of the Research on Water landing of Manned Space Vehicle", JSASS 56th Space Sciences and Technology Conference, 3G05, 2012. (in Japanese).
[7] R. Sugimoto, E. Nakano, H. Uchikawa, H. Tanno and T. Shimoda, "Water Landing Simulation of Slow-Descending Capsule", JSASS 57th Space Sciences and Technology Conference, 2J04, 2013. (in Japanese)
[8] E. Nakano, H. Uchikawa, H. Tanno, T. Imada, H. Akagi, T. Seki, T. shimoda and R. Sugimoto, "Overview of the Research on Water Impact of Reentry manned Space Capsule",JSASS 57th Space Sciences and Technology Conference, 2J03, 2013. (in Japanese)
[9] H. Tanno, T. Komuro, K. Sato, K. Itoh and M. Takahashi, "Miniature data-logger for aerodynamic force measurement in impulsive facility", AIAA 2010-4204, 2010.
[10] E. Fasanelle, "Multi-Terrain Earth Landing Systems Applicable for Manned Space Capsules", ASCE 11th Earth and Space Conference, 2008.